Journal of Hazardous Materials 190 (2011) 442–450

Contents lists available at ScienceDirect

Journal of Hazardous Materials

journal homepage: www.elsevier.com/locate/jhazmat

Sorption of uranium(VI) using oxime-grafted ordered mesoporous carbon CMK-5

Gan Tian, Junxia Geng, Yongdong Jin, Chunli Wang, Shuqiong Li, Zhen Chen, Hang Wang, Yongsheng Zhao, Shoujian Li *

College of Chemistry, Sichuan University, Chengdu 610064, PR China

ARTICLE INFO

Article history:
Received 3 September 2010
Received in revised form 22 February 2011
Accepted 18 March 2011
Available online 29 March 2011

Keywords:
Uranium
CMK-5
Oxime
Diazotization
Sorption

ABSTRACT

A new sorbent for uranium(VI) has been developed by functionalizing ordered mesoporous carbon CMK-5 with 4-acetophenone oxime via thermally initiated diazotization. The sorption of U(VI) ions onto the functionalized CMK-5 (Oxime-CMK-5) was investigated as a function of sorbent dosage, pH value, contact time, ionic strength and temperature using batch sorption techniques. The results showed that U(VI) sorption onto Oxime-CMK-5 was strongly dependent on pH, but to a lesser extent, on ionic strength. Kinetic studies revealed that the sorption process achieved equilibrium within 30 min and followed a pseudo-first-order rate equation. The isothermal data correlated with the Langmuir model better than the Freundlich model. Thermodynamic data indicated the spontaneous and endothermic nature of the process. Under current experimental conditions, a maximum U(VI) sorption capacity was found to be 65.18 mg/g. Quantitative recovery of uranium was achieved by desorbing the U(VI)-loaded Oxime-CMK-5 with 1.0 mol/L HCl and no significant decrease in U(VI) sorption capability of Oxime-CMK-5 was observed after five consecutive sorption–desorption cycles. The sorption study performed in a simulated nuclear industry effluent demonstrated that the new sorbent showed a desirable selectivity for U(VI) ions over a range of competing metal ions.

1. Introduction

Over the past few decades, a variety of technologies have been developed for the removal and recovery of uranium present in nuclear fuel effluents, mine tailings, seawater, and other waste sources in consideration of the dual significance of uranium, the potential environmental health threat and an nonrenewable resource of nuclear energy [1]. Recently, solid–liquid separation technique based on carbonaceous materials, such as activated carbon [2–5], carbon nanotubes [6,7] and carbon fiber [8] has been gradually applied to this area. The carbonaceous materials have been chosen for this purpose because of their higher thermal and radiation resistance than organic exchanger resins and better acid–base stability compared with familiar inorganic sorbents [2,5].

Moreover, as a new member of the carbonaceous material family, the ordered mesoporous carbon CMK-5, which is synthesized through the nanocasting technique [9], has attracted considerable attention because of its unique features, such as high surface area, regular mesoporous pore structure, narrow pore size distribution, large pore volume, as well as excellent chemical and physical stabilities [10,11]. These features make CMK-5 more attractive as catalyst supports, electrode materials and energy storage media [12–14]. However, to the best of our knowledge, CMK-5 has not been reported for separation of uranyl ions and/or other metal ions from aqueous system so far. Therefore, it would be interesting to explore the possibility of preparing a new sorbent based on the porous carbon for the environmental purpose mentioned above.

Although the pristine CMK-5 itself, as with most of other carbonaceous materials, shows almost no selectivity in metal ions sorption based on the results of pre-experiments in our lab, chemical modification via grafting specific chelating ligands onto the matrix would make it possible for the porous carbon to selectively adsorb uranium.

An efficient route for covalent binding organic functional groups to carbon surface is diazotization, through which benzene-substituted motifs can be directly grafted to carbon surface via electrochemical reduction of diazonium salts [15,16] or in situ chemical modification by diazonium compounds [17,18]. The general principle of diazotization (Scheme is omitted for brevity) presents that once the diazonium compound forms, it would decompose instantaneously and give a reactive phenyl radical (under electrochemical reduction) or a phenyl cation (under non-electrochemical reduction), which abstracts the active hydrogen atom from the carbon surface and then covalently attaches to the surface. Compared with the conventional chemical modification of

* Corresponding author at: College of Chemistry, Sichuan University, 29# Wangjiang Lu, Chengdu 610064, PR China. Tel.: +86 28 85412329; fax: +86 28 85412907.
E-mail address: sjli000616@scu.edu.cn (S. Li).

0304-3894/$ – see front matter © 2011 Elsevier B.V. All rights reserved.
doi:10.1016/j.jhazmat.2011.03.066

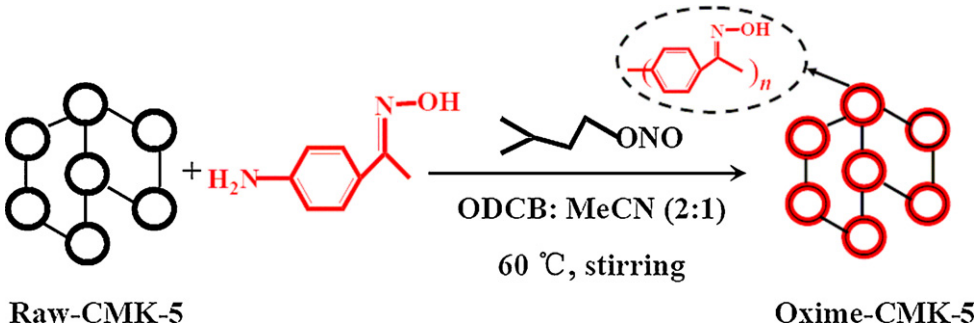

Scheme 1. Functionalization of CMK-5 with oxime groups through diazotization.

carbon surface involving oxidation based on strong oxidizing acids and/or oxidizers, diazotization method could simplify the grafting procedure, singularize the target functional group introduced on the carbon surface as designed, and furthermore, avoid deterioration in mechanical strength and surface smoothness associated with the oxidation [15].

Again, oxy-imines, >C=N–OH, also abbreviated as oximes, constitute an important class of chelating agents. They have found extensive applications as highly selective reagents for the separation/detection of a diversity of metal ions [19]. For instance, salicylaldoxime has been employed for liquid–liquid extraction of uranium(VI) from weakly acidic solutions, and the ion imprinted polymer loading this complexing ligand could also selectively remove the UO_2^{2+} from synthetic nuclear power reactor effluents [20]. In addition, numerous researches on amidoxime modified polymers employed for selective enrichment of uranium(VI) from aqueous system have also been reported [21–23]. In view of these, it would be a significant attempt to anchor an oxime-containing ligand onto CMK-5 to offer an efficient sorbent for selective separation of U(VI) ions from various aqueous solutions.

In the present work, 4-acetophenone oxime was covalently immobilized onto the ordered mesoporous carbon CMK-5 through the thermally induced reaction on the matrix with in situ generated diazonium compounds in organic solvent medium. The functionalized CMK-5 (Oxime-CMK-5) was characterized and its sorption behavior of U(VI) ions was investigated in detail using batch equilibrium methods under varying operating conditions.

2. Experimental

2.1. Materials

2.1.1. Sorbent preparation

An ordered mesoporous silica SBA-15 (Al-SBA-15) employed as the hard template in this study was synthesized according to the reference reported [24], and the CMK-5 carbon samples (named as Raw-CMK-5) were obtained by following procedure described elsewhere [12]. In a typical procedure (see Scheme 1), 0.60 g (50 mmol) pristine CMK-5 and 60 mL 1,2-dichlorobenzene (ODCB) were added in a three-necked flask equipped with a reflux condenser and a magnetic stir bar. The mixture was stirred for 30 min at room temperature to obtain a homogenous dispersion, and to this suspension was added a solution of the as-synthesized 4-aminoacetophenone oxime [25] (0.75 g, 5 mmol) in 30 mL acetonitrile. After cautious, slow addition of 1.7 mL (6 mmol) isoamyl nitrite, the reaction system was heated at 60 °C for 10 h with stirring, and then cooled to room temperature. The suspension was filtered and washed with dimethylfomamide (DMF) until the filtrate became colorless. The collected solid was washed with DMF for further purification through repeated sonication and finally washed by anhydrous ethanol, then dried at 70 °C in a vacuum oven for 12 h. The resulting material was denoted as Oxime-CMK-5.

2.1.2. U(VI) stock solution and the simulated nuclear industry effluent sample preparation

A stock uranium(VI) solution (~1000 mg/L) was prepared by dissolving appropriate amounts of standard U_3O_8 in nitric acid aqueous solution, the single U(VI) working solutions (25–300 mg/L) were prepared by appropriate dilution of the stock solution. The simulated nuclear industry effluent sample was prepared according to the main components in nuclear industry effluent samples from a local factory and the components involved are listed in Table 1.

All chemicals used were of analytical grade or better and used without further purification. All testing solutions were prepared with deionized water.

2.2. Apparatus

Infrared spectra (FTIR) were recorded with Perkin-Elmer IR-843 spectrometer (USA). CHN content was determined by the elemental-analysis device (CARLO 1106, Italy). Surface topography of the Raw-CMK-5 and Oxime-CMK-5 were observed by a scanning electron microscope (SEM, Philips XL-3, Netherlands). Surface area and pore size distribution were obtained by a N_2 adsorption–desorption device (ZXF-6, China). Thermal stability and the functional group content of Oxime-CMK-5 was inspected using a TGA meter (SDT Q600, USA).

2.3. Batch sorption studies

Studies on the U(VI) sorption behavior were performed on Oxime-CMK-5, and/or Raw-CMK-5 if needed, in batch experiments using 50 mL Erlenmeyer flasks. The effect of sorbent dosage, pH, equilibrium time, ionic strength, temperature and competing ions were examined. Equilibrium studies were conducted within the U(VI) concentration range of 25–300 mg/L. Solution pH was adjusted and measured on a digital pH-meter (PHS-4CT, China)

Table 1
Composition of the simulated nuclear industry effluent sample.

Coexistent ions	Added as	Concentration (mg/L)
Na^+	NaCl	162.15
Co^{2+}	$CoCl_2{\cdot}6H_2O$	119.26
Ni^{2+}	$Ni(NO_3)_2{\cdot}6H_2O$	123.55
Mn^{2+}	$MnCl_2{\cdot}4H_2O$	113.73
Zn^{2+}	$ZnCl_2$	124.62
Sr^{2+}	$SrCl_2{\cdot}6H_2O$	194.27
Ce^{3+}	$Ce(NO_3)_3{\cdot}6H_2O$	254.10
Cr^{3+}	$CrCl_3{\cdot}6H_2O$	85.56
La^{3+}	$LaCl_3{\cdot}nH_2O$	273.53
UO_2^{2+}	U_3O_8	180.90

Sample solution conditions: pH = 4.0 and T = 283.15 K.

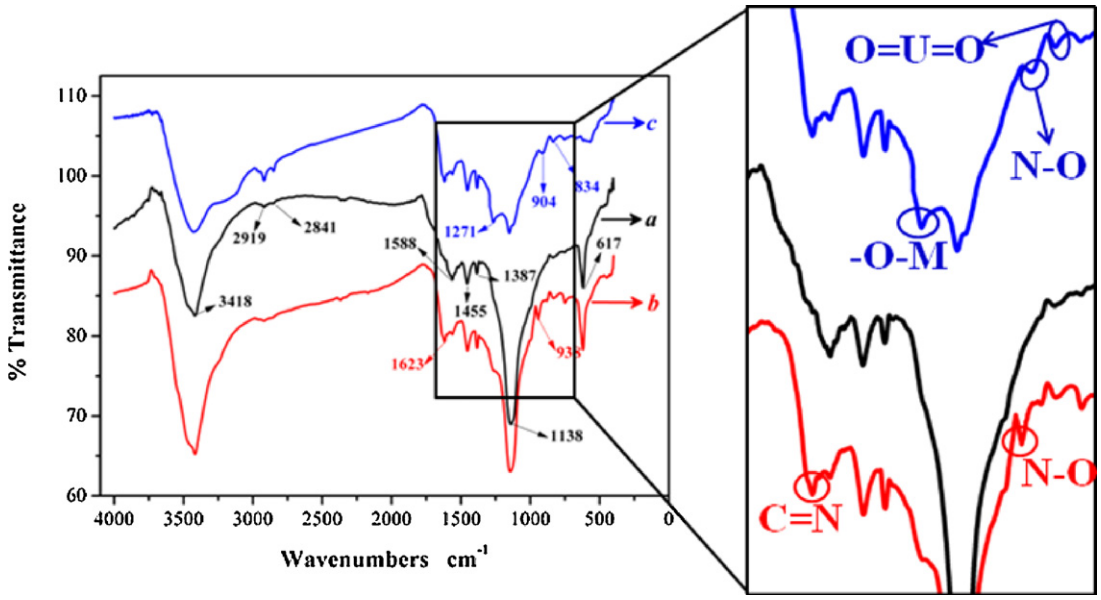

Fig. 1. Infrared spectrum of (a) Raw-CMK-5, (b) Oxime-CMK-5, and (c) UO_2^{2+}-Oxime-CMK-5.

using HNO_3 and NaOH solution, and the ionic strength was adjusted by adding a required amount of sodium chloride. Detailed experimental conditions are presented in the related figure captions for clear identification. The solutions were withdrawn from the flasks and separated from the solids by centrifugation, then the initial and the residual concentration of tested ion(s) in supernatants were determined by inductively coupled plasma atomic emission spectroscopy (ICP-AES, Thermo Elemental, USA). The sorption amount q_e (mg/g) of adsorbed uranyl ions and/or other metal ions is calculated as:

$$q_e = \frac{(C_0 - C_e) \times V}{m} \quad (1)$$

The distribution coefficient K_d is a specific value measuring the sorbent's sorption capability.

$$K_d = \frac{C_0 - C_e}{C_e} \times \frac{V}{m} \quad (2)$$

where C_0 (mg/L) is the initial concentration of metal ion, C_e (mg/L) is the equilibrium concentration, V (L) is the volume of the testing solution and m (g) is sorbent dose.

2.4. Desorption and reusability studies

In each desorption experiment, 20 mg of the spent sorbent was treated with 25 mL of various concentration HCl solution, allowed to equilibrate for 2 h, then centrifuged for solid–liquid separation and finally U(VI) content in the supernatant was determined. The spent sorbents for this study were prepared by equilibrating 0.25 g Oxime-CMK-5 with 100 mL U(VI) solution (200 mg/L, pH = 4.5) for 2 h at 200 rpm and 283.15 ± 1 K in an isothermal shaker bath. Desorption efficiency is expressed as:

$$\text{Desorption}\,(\%) = \frac{\text{Amount of U(VI) desorbed}}{\text{Amount of U(VI) adsorbed}} \times 100 \quad (3)$$

To determine the reusability of Oxime-CMK-5, consecutive sorption–desorption cycles were repeated for 5 times with the same sorbent using fresh U(VI) solution (100 mg/L, pH = 4.5) at 283.15 ± 1 K. Regeneration of the sorbent was carried out using 1.0 mol/L HCl.

All experimental series were performed at least twice.

3. Results and discussion

3.1. Characterization

3.1.1. FTIR

Fig. 1 shows the FT-IR spectra of Raw-CMK-5, Oxime-CMK-5 and U(VI) adsorbed Oxime-CMK-5 (denoted as UO_2^{2+}-Oxime-CMK-5). For all samples, the peak at 3418 cm^{-1} is assigned to the –OH stretching vibration arising from physically adsorbed water or surface hydroxyl groups on the adsorbent. The two characteristic bands at 2841 and 2919 cm^{-1} can be assigned to C–H stretching, and the peak at 1138 cm^{-1} can be assigned to CH–O–CH_2 [7]. In addition, the three absorption bands emerging at 1588, 1455 and 1387 cm^{-1} are due to benzene-ring vibrations, which also contain one more sharp band at 617 cm^{-1} ascribed to out of plane ring C–H bending vibration [5]. In comparison to the spectrum of Raw-CMK-5 (Fig. 1a), the additional absorption peaks at 1623 cm^{-1} and 938 cm^{-1} observed in the spectrum of Oxime-CMK-5 (Fig. 1b) correspond to the stretching vibration of C=N and N–O, respectively [19–23], clearly stating that the designed oxime-containing groups have been efficiently attached to the carbon surface. After U(VI) sorption onto Oxime-CMK-5, the characteristic peak of UO_2^{2+} has been clearly observed at 834 cm^{-1} in Fig. 1c [20,23], which confirms the sorption of UO_2^{2+} on Oxime-CMK-5. Furthermore, a shift of N–O stretching from 938 cm^{-1} to 904 cm^{-1} has been detected [22] and a new band centered at 1271 cm^{-1}, the characteristic band for –O–M bond [21,22] due to the complexation of Oxime-CMK-5 with UO_2^{2+} through N–O– group also has been observed. These results might suggest that the oxime groups coordinate with UO_2^{2+}, as shown in Scheme 2.

3.1.2. TGA

Thermal analysis was performed for Oxime-CMK-5 sample and the result is shown in Fig. 2. The weight loss below 150 °C (ca. 4.5 wt%) could be attributed to physically adsorbed water. Further, at temperatures above 300 °C, the rate of weight loss sharply increased owing to pyrolysis of the grafted functional groups. The most significant weight loss occurred in the temperature range of 300–600 °C, suggesting stable covalent bonding of the oxime functional groups to the CMK-5 surface. At or near 600 °C, the total weight loss reaches about 28.9%, from which the grafting ratio could

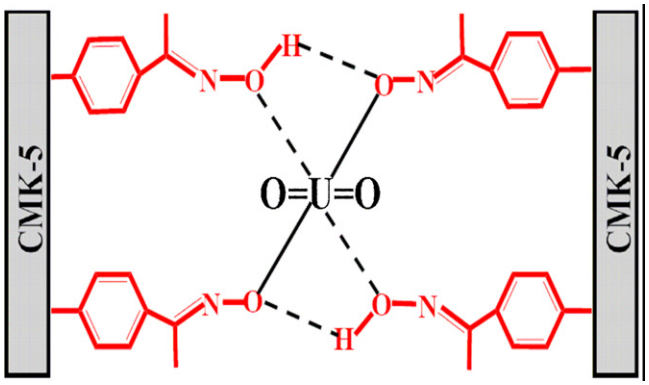

Scheme 2. The supposed UO_2^{2+}-Oxime complex formation.

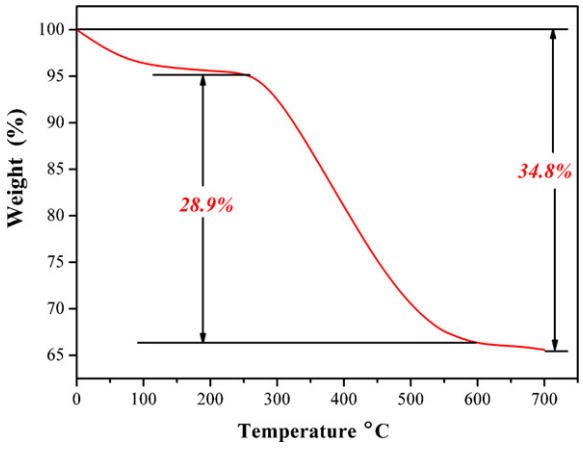

Fig. 2. TGA profile for Oxime-CMK-5 (10 °C/min, N_2 atmosphere).

be calculated as 2.16 mmol/g. The result is in agreement with the corresponding data (2.14 mmol/g) evaluated by the fluctuation of N content between Raw-CMK-5 and Oxime-CMK-5 through CHN element analysis (see Table 2). The TGA profile confirms that a significant amount of the functional groups have been chemically grafted on the carbon surface, and the resulting material has excellent thermal stability.

Table 2
CHN content of Raw-CMK-5 and Oxime-CMK-5.

Samples	C%	N%	H%
Raw-CMK-5	89.57	0.34	2.21
Oxime-CMK-5	81.60	3.34	2.47

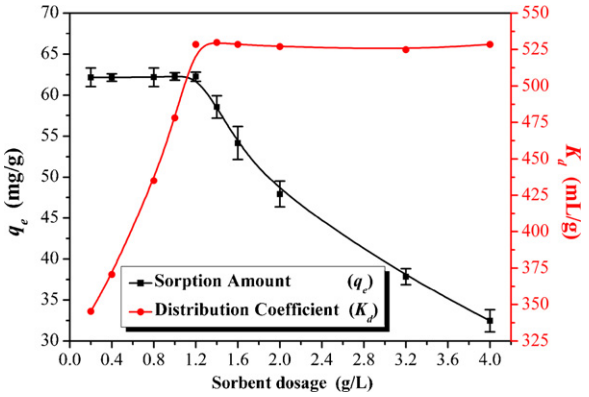

Fig. 4. Effect of sorbent dosage on the U(VI) uptake by Oxime-CMK-5, C_0 = 200 mg/L, pH = 4.5, t = 120 min and T = 283.15 K.

3.1.3. BET surface and pore structure

The results of the nitrogen adsorption–desorption experiments showed that Raw-CMK-5 possessed a uniform pore size distribution centered at 8.30 nm. But after diazotization, pore diameter of Oxime-CMK-5 decreased and centered at 4.53 nm. Correspondingly, surface area and pore volume decreased from 992.0 m^2/g and 0.78 cm^3/g to 578.7 m^2/g and 0.52 cm^3/g, respectively. Taking into account the fact that after sufficient washing, almost no excess reactants attached on the surface of the resulting material, the decrease in surface area, pore size and pore volume after diazotization would be attributed to the effective graft-functionalization, that is, the grafted functional groups uniformly dispersed on the external and internal surface occupied portion of the pore volume and area of the porous matrix.

3.1.4. SEM

SEM images presented in Fig. 3a and b demonstrated that the oxime functionlization did not bring any noticeable damage to the surface morphology of Oxime-CMK-5 since the surface did not show any serious cracks or deformation as compared with that of Raw-CMK-5. Moreover, SEM image in Fig. 3c showed that the surface of UO_2^{2+}-Oxime-CMK-5 became a little bit rougher, but it still maintained uniform rod-like morphology after sorption of U(VI).

3.2. Sorption behavior studies

3.2.1. Effect of sorbent dosage

In Fig. 4, the contrary trends could be observed for the two curves associated with sorption amount q_e and distribution coefficient K_d. Under the test condition, the maximum values of q_e observed were about 65 mg/g in the initial part, whereas the corresponding K_d gradually reached to a fixed value at about 530 mL/g in the later part. As a result, the knee points of the two curves were found

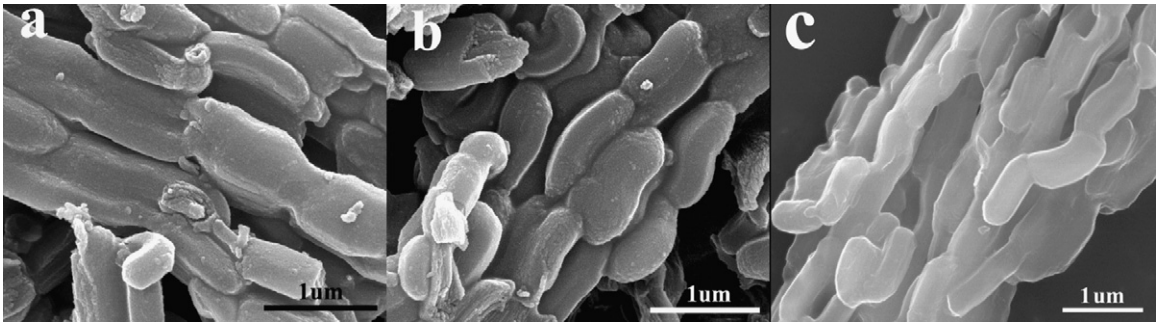

Fig. 3. SEM images of (a) Raw-CMK-5, (b) Oxime-CMK-5, and (c) UO_2^{2+}-Oxime-CMK-5.

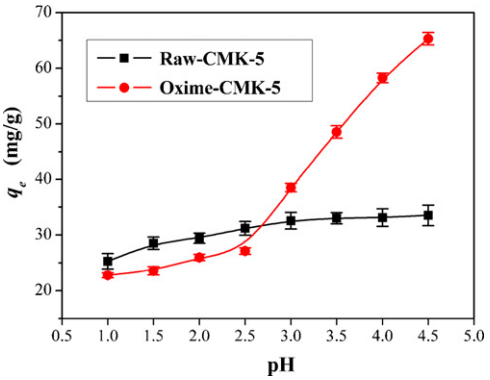

Fig. 5. Effect of pH on the U(VI) uptake by Raw-CMK-5 and Oxime-CMK-5, C_0 = 200 mg/L, t = 120 min and T = 283.15 K.

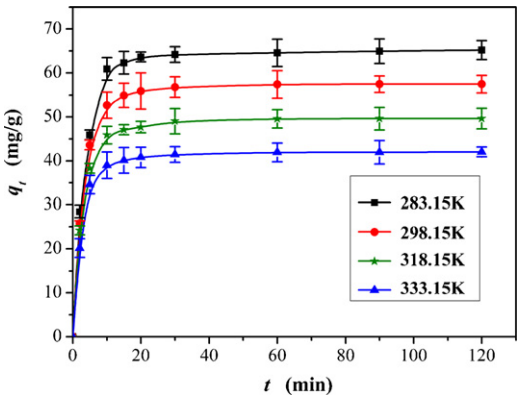

Fig. 6. Effect of contact time on the U(VI) uptake by Oxime-CMK-5, C_0 = 200 mg/L and pH = 4.5.

locating just at the solid/liquid ratio of 1.2 g/L. Therefore, 1.2 g/L was chosen as the suitable dosage during the following batch tests.

3.2.2. Effect of pH

The effect of pH on the U(VI) sorption capability of Raw-CMK-5 and Oxime-CMK-5 was investigated and pH value was limited within 4.5 in case that the soluble form of U(VI) ions would be converted into insoluble species according to solubility calculation [26,27]. As shown in Fig. 5, the subdued curve expressed that the uptake of U(VI) ions on Raw-CMK-5 was hardly influenced by pH for its relatively immaculate surface inactive to H^+. While the other soaring curve revealed that the U(VI) sorption increased steadily between pH 1 and 2.5, but sharply when the solution pH was changed beyond 2.5, clearly stating that U(VI) sorption on Oxime-CMK-5 was strongly pH dependent.

The remarkable influence of pH on the sorption capacity suggests that the sorption of UO_2^{2+} onto Oxime-CMK-5 is dominated by surface complexation. It is well known that the chealting group on Oxime-CMK-5 can perform differently along with the changes in pH owing to its protonation or deprotonation behavior [19,22,23]. At low pH values, the hydroxyl groups of oxime on Oxime-CMK-5 will be highly protonized, resulting in decreasing the oxime's nucleophilicity towards U(VI) and limiting the U(VI) sorption onto the sorbent. As the pH values increase, the protonation degree of the oxime groups will be reduced and the hydroxyl proton in oxime group would be easier to strip off, allowing the lone-pair electron on the negative charged oxygen more prone to occupy the empty orbits of the uranium atom, and consequently favoring the formation of the complex as shown in Scheme 2.

3.2.3. Kinetics study

As seen from Fig. 6, it is evident that the sorption of U(VI) ions appeared to take place in two distinct steps: a relatively fast one continuing up to 10 min followed by a slower one to the equilibrium state. A fast U(VI) sorption kinetics was revealed in this system and the necessary time to reach the equilibrium was about 30 min. The high initial uptake rate is due to the higher active site availability for U(VI) sorption at the onset of the process. In addition, structural properties of the highly ordered mesoporous matrix allow the U(VI) ions to be able to penetrate through the pores more easily, which is known as intra-particle diffusion [28], and get adsorbed at active sites on the pore surfaces.

Two kinetic models namely pseudo-first-order and pseudo-second-order models were employed to describe the sorption process. The linear form of the two models can be expressed as followed, respectively [29,30].

The pseudo-first-order equation : $$\ln(q_e - q_t) = \ln q_e - k_1 t \quad (4)$$

The pseudo-second-order equation : $$\frac{t}{q_t} = \frac{1}{k_2 q_e^2} + \frac{t}{q_e} \quad (5)$$

where q_t and q_e are the amounts of U(VI) ions adsorbed (mg g^{-1}) at time t (min) and at equilibrium time, respectively; k_1 (min^{-1}) and k_2 (g mg^{-1} min^{-1}) are the pseudo-first-order and the pseudo-second-order sorption rate constant, respectively. In Eq. (5), the expression $k_2 q_e^2$ in the intercept term describes the initial sorption rate, r (g mg^{-1} min^{-1}) as $t \to 0$.

$$r = k_2 q_e^2 \quad (6)$$

Data generated from batch studies were investigated by the two models (figures are omitted for brevity) and kinetic parameters listed in Table 3 implied that the U(VI) sorption here could be better represented by the pseudo-first-order kinetic model in view of its higher correlation coefficients, moreover, the q_e values calculated by the model are closer to those obtained by experiments. The activation energy (E_a) calculated using the Arrhenius equation [2] was found to be 9.36 kJ/mol, indicating a chemical sorption progress.

As mentioned above, intra-particle diffusion may contribute to the initial high uptake rate. The results were further subjected to analysis by the intra-particle diffusion model, since neither the pseudo-first-order nor the pseudo-second-order model can evaluate the diffusion mechanism and rate-determining step. The model devised by Weber and Moris [28] is expressed as:

$$q_t = k_{id} t^{0.5} \quad (7)$$

where k_{id} is the intra-particle diffusion rate constant. This model predicts that the plot of q_t versus $t^{0.5}$ should be linear and pass through the origin if adsorption of an adsorbate from aqueous solution is controlled by the intra-particle diffusion process. The results in Fig. 7 showed that the relationship between q_t and $t^{0.5}$ is not linear for the entire range of reaction time, suggesting the intra-particle diffusion was not the only rate-controlling step. Specifically, it could be divided into three straight parts, which indicated that three types of mechanisms might be involved in the sorption process [28]. Initial rapid uptake rate due to immobilizing U(VI) ions to active sites on external surface was controlled by surface adsorption, once reached the saturation, the U(VI) ions began to enter into Oxime-CMK-5 particles via the pores and were adsorbed by the interior surface, where intra-particle diffusion was the rate-determining step, and then the adsorption equilibrium was reached as the intra-particle diffusion started to slow down. Therefore, both the surface adsorption as well as intra-particle diffusion may contribute to the rate-determining step during the process of U(VI) uptake by Oxime-CMK-5. The intra-particle diffusion rate (Table 3) obtained from the slope of the steep-sloped

Table 3
Kinetic parameters for U(VI) sorption onto Oxime-CMK-5.

Parameters	T (K)			
	283.15	298.15	313.15	333.15
q_e (exp) (mg g^{-1})	64.66	57.47	49.60	42.04
Pseudo-first-order model				
k_1 (min^{-1})	0.243	0.298	0.365	0.448
R^2	0.9988	0.9956	0.9956	0.9968
q_e (cal) (mg g^{-1})	60.46	53.89	46.72	39.33
Error (%)	−6.50	−6.21	−5.81	−6.45
Pseudo-second-order model				
k_2 (g mg^{-1} min^{-1})	3.91×10^{-3}	5.07×10^{-3}	6.92×10^{-3}	10.47×10^{-3}
R^2	0.9762	0.9801	0.9735	0.9646
r (mg g^{-1} min^{-1})	21.29	23.58	24.09	25.00
q_e (cal) (mg g^{-1})	73.75	68.21	59.00	48.92
Error (%)	+14.40	+18.96	+18.95	+16.37
Intra-particle diffusion model				
k_{id} (mg g^{-1} min$^{-0.5}$)	19.48	17.16	14.89	12.67
R^2	0.9963	0.9761	0.9698	0.9716

Initial concentration of U(VI) = 200 mg/L, pH = 4.5; Error(%)= $[q_e(\text{cal}) - q_e(\text{exp})]/q_e(\text{exp}) \times 100$.

part indicated that lower temperature was more favorable for the diffusion and transportation of U(VI) ions into sorbent pores.

3.2.4. Isotherm modeling

The equilibrium experiments were performed with samples of varying initial U(VI) concentration from 25 to 300 mg/L, and the pH value was selected at 4.0 in order to avoid the occurrence of insoluble U(VI) species. The results in Fig. 8 expressed that all of the four curves displayed a continuous increase of U(VI) uptake with the increase of residual U(VI) concentration until equilibrium was reached, indicating Oxime-CMK-5 should have a limited sorption capacity. In addition, the sorption capacity decreased with the increase of temperature, revealing that the sorption process is an exothermic process in nature. Under the current experimental conditions, the maximal sorption capacity was about 0.25 mmol/g at 283.15 K, which was unexpected as the higher grafting ratio (2.16 mmol/g) determined from the TGA and CHN element analysis suggested that the sorbent could have greater adsorption capability. However, the sorption capacity was generally affected by numerous factors, among which pH would always be a predominant process parameter, since the sorption process was obviously affected by the protonation/deprotonation of the oxime hydroxyl groups on the sorbent, especially at lower pH value. Moreover, 4-fold coordination structure as illustrated in Scheme 2 might partly account for the big difference between the U(VI) sorption capacity and the grafting density of oxime groups on CMK-5.

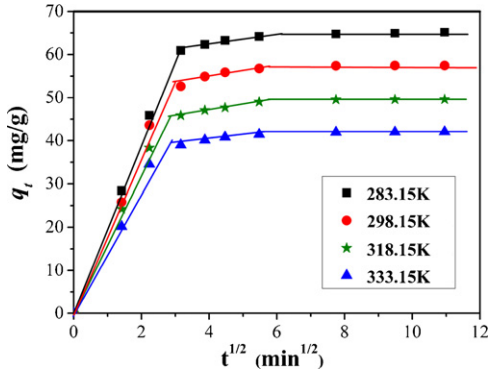

Fig. 7. Intra-particle diffusion model fitting plots for the U(VI) uptake by Oxime-CMK-5, C_0 = 200 mg/L and pH = 4.5.

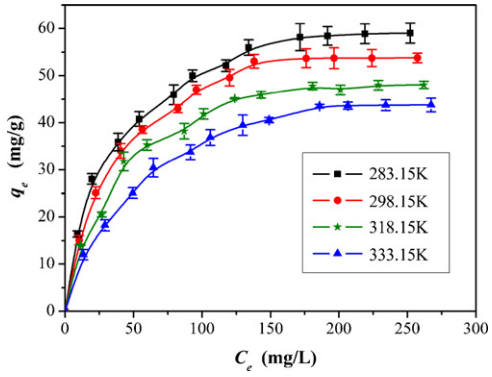

Fig. 8. Equilibrium isotherms for U(VI) sorption onto Oxime-CMK-5, pH = 4.0 and t = 120 min.

The equilibrium data were modeled using the two frequently used isotherm models, namely Langmuir and Freundlich isotherms, to explain the experimental results and the real sorption behavior.

The Langmuir model assumes that the removal of metal ions occurs on an energetically homogenous surface by monolayer sorption and there are no interactions between the adsorbates on adjacent sites. The linear equation of the Langmuir sorption model [31] is expressed by:

$$\frac{C_e}{q_e} = \frac{1}{bq_m} + \frac{C_e}{q_m} \tag{8}$$

The Freundlich isotherm model is an empirical relationship describing the sorption of solutes from a liquid to a solid surface and assumes that different sites with several sorption energies are involved, which linear equation is given by [32]:

$$\ln q_e = \ln K_F + \frac{1}{n} \ln C_e \tag{9}$$

where q_e (mg/g) and C_e (mg/L) are the equilibrium concentrations of U(VI) in the solid and liquid phase, respectively, q_m (mg/g) is the measure of Langmuir monolayer sorption capacity and b (L/mg) is the equilibrium constant. K_F [mg/g (L/mg)$^{1/n}$] and n are characteristic constants related to the relative sorption capacity of the sorbent and the intensity of sorption, respectively.

The fitting plots are omitted here for brevity, the correlation coefficients (R^2) and corresponding parameters are presented in Table 4. It could be found that both of the two models fitted well according to the high correlation coefficients ($R^2 > 0.95$). Higher correlation coefficients expressed the Langmuir isotherm fitted better to the sorption data, indicating that Oxime-CMK-5 provided the specific homogeneous sites and sorption of U(VI) ions onto Oxime-CMK-5 generated monolayer. In that case, Oxime-CMK-5 should have a limited sorption capacity.

Table 4
The Langmuir and Freundlich model parameters of U(VI) sorption onto Oxime-CMK-5.

T/K	q_e (mg/g)	Langmuir isotherm			Freundlich isotherm		
		q_m (mg/g)	b (L/mg)	R^2	K_F, (mg/g (L/mg)$^{1/n}$)	n	R^2
283.15	57.19	65.40	0.0192	0.9961	7.681	2.47	0.9613
298.15	51.74	62.00	0.0252	0.9983	6.251	2.32	0.9556
318.15	46.15	57.80	0.0303	0.9924	5.052	2.22	0.9514
333.15	40.75	53.90	0.0338	0.9952	2.575	2.04	0.9758

Initial concentration of U(VI) = 200 mg/L, pH = 4.0; q_e: U(VI) sorption capacity at equilibrium state from experiments.

The Langmuir parameter b can be used to predict the affinity between the adsorbate and sorbent using the separation factor R_L [5].

$$R_L = \frac{1}{1 + bC_0} \tag{10}$$

R_L values were calculated (presented in Supplementary data) and found to lie in the range of 0–1 (as the value of b is positive) demonstrating a favorable and irreversible sorption process. Again, higher R_L values at lower metal concentrations showed that U(VI) sorption was more favorable at lower concentrations.

3.2.5. Effect of ionic strength

Ionic strength was adjusted by varying NaCl concentration and the results in Fig. 9 showed that the amount of U(VI) ions adsorbed decreased as the ionic strength increased. Higher ionic strength created a higher shielding effect for U(VI) ions adsorbing onto the Oxime-CMK-5 surface, which caused a decrease in sorption; on the other hand, the competition between increasing Na^+ ions and U(VI) ions for the active sites on Oxime-CMK-5 might also be responsible for the decrease. In addition, McBride indicates that ions that form outer-sphere complexes show decrease in sorption with increasing ionic strength, whereas inner-sphere complexes are not [33]. Thus in the case of U(VI) sorption by Oxime-CMK-5, outer-sphere surface complex formation could be considered to describe the decrease of U(VI) sorption.

3.2.6. Thermodynamic study

The U(VI) sorption onto Oxime-CMK-5 was investigated at four different temperatures, together with two different pH values and two initial U(VI) concentrations. As seen in Fig. 10a, the trends of U(VI) sorption capacity, in all cases, showed a continuous decrease with increasing temperature, which suggested that the lower temperature would be more favorable for effective U(VI) sorption. Furthermore, the higher sorption capacity at higher pH with the same initial concentration again confirmed the U(VI) sorption onto Oxime-CMK-5 was pH-dependence.

To evaluate the thermodynamic feasibility and understand the nature of the sorption process, three basic thermodynamic parameters, standard free energy (ΔG°), standard enthalpy (ΔH°) and standard entropy (ΔS°), were calculated using the following equations [5].

$$\Delta G^\circ = \Delta H^\circ - T\Delta S^\circ \tag{11}$$

$$\ln K_d = \frac{\Delta S^\circ}{R} - \frac{\Delta H^\circ}{RT} \tag{12}$$

Values of ΔH° and ΔS° were calculated from the plots K_d versus $1/T$ (Fig. 10b) and listed in Table 5 along with the values of ΔG° appraised using Eq. (11). The negative values of ΔH° conform that the sorption process is exothermic. The negative values of ΔS° infer a decrease in randomness from the sorption of U(VI) ions to the active sites on the sorbent. The spontaneous nature of the sorption process is evidenced by the negative values of ΔG°. Furthermore, the less negative values of ΔG° at higher temperature suggest that the bonding between U(VI) ions and active sites on the sorbent are less stable at higher temperature and the U(VI) sorption process becomes more favorable at lower temperatures.

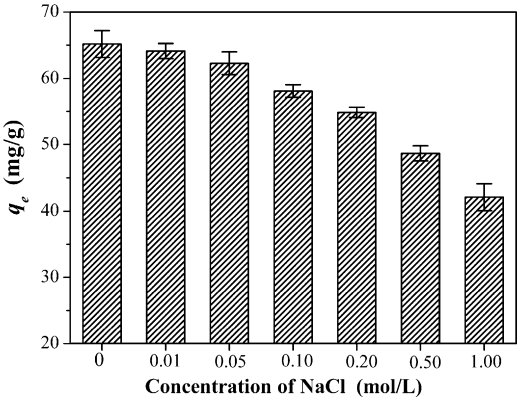

Fig. 9. Effect of ionic strength on the U(VI) uptake by Oxime-CMK-5, C_0 = 200 mg/L, pH = 4.5, t = 120 min and T = 283.15 K.

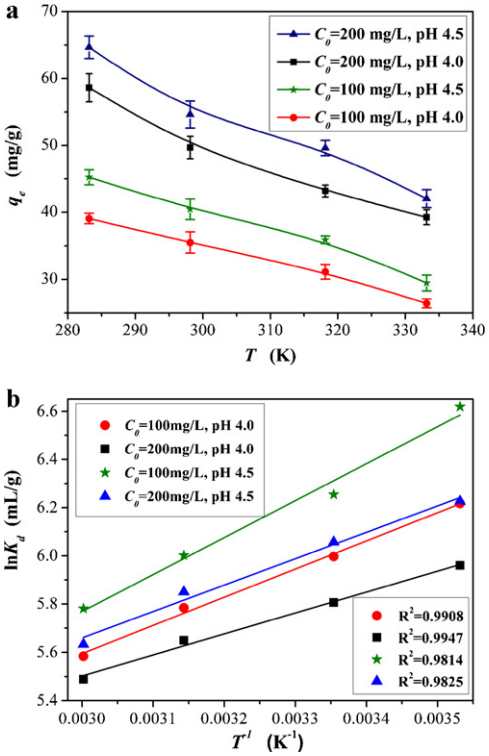

Fig. 10. (a) Effect of temperature on the U(VI) uptake by Oxime-CMK-5, t = 120 min and (b) plots of ln K_d versus $1/T$ for the U(VI) sorption onto Oxime-CMK-5.

Table 5
Thermodynamic parameters for U(VI) sorption onto Oxime-CMK-5.

C_0 (mg/L)	pH	ΔH° (kJ/mol)	ΔS° (J/(mol K))	ΔG° (kJ/mol)			
				283.15 K	298.15 K	318.15 K	333.15 K
100	4.5	−22.54	−24.10	−15.71	−15.35	−14.87	−14.51
	4.0	−19.54	−18.57	−14.28	−14.00	−13.63	−13.35
200	4.5	−18.96	−15.99	−14.43	−14.19	−13.87	−13.63
	4.0	−17.09	−12.02	−13.69	−13.51	−13.27	−13.09

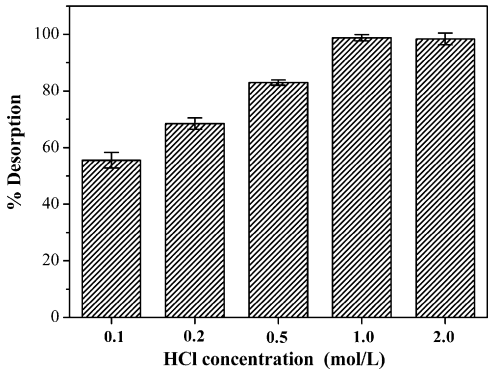

Fig. 11. Effect of HCl concentration on U(VI) desorption.

3.3. Desorption and reusability study

As illustrated in Fig. 5, smaller U(VI) uptake by Oxime-CMK-5 was observed at a lower pH range, which implies that adsorbed U(VI) ions can be desorbed from spent sorbent by an acid medium. Desorption tests were tried with HCl solutions in the concentration range from 0.1 to 2.0 mol/L. The results presented in Fig. 11 demonstrated higher acidity promoted the desorption progress. Reusability experiments were conducted adopting 1.0 mol/L HCl as desorbing agent and the results are shown in Table 6. After five consecutive sorption/desorption cycles, the sorption capability decreased from 99.2 ± 2.5 in the first cycle to 97.4 ± 3.2% in the fifth cycle, while the recovery of U(VI) ions decreased from 97.5 ± 1.8% to 94.1 ± 0.9%. The results indicated the U(VI)-loaded Oxime-CMK-5 could be efficiently regenerated by 1.0 mol/L HCl and reused with only slight impact on its U(VI) sorption capability after 5 cycles.

3.4. Test with a simulated nuclear industry effluent

The simulated nuclear industry effluent was treated with Raw-CMK-5 and Oxime-CMK-5 under batch tests. The results in Fig. 12a showed that the chemical modification brought an obvious increase in U(VI) sorption capability. The total sorption capacity of Oxime-CMK-5 achieved 0.58 mmol/g, 32% higher than that of Raw-CMK-5 (0.44 mmol/g). Significantly, more than 70% of the increment was contributed by the additional U(VI) sorption, which suggested the Oxime-CMK-5 had markedly higher affinity to U(VI) ions.

Table 6
Five cycles of the U(VI) sorption/desorption with 1.0 mol/L HCl solution as the desorbing agent.

Cycles number	Sorption		Desorption (%)
	q_e (mg/g)	%	
1	44.76 ± 1.13	99.2 ± 2.5	97.5 ± 1.8
2	45.16 ± 1.98	100.1 ± 4.4	96.4 ± 3.3
3	44.57 ± 1.05	98.8 ± 2.4	96.9 ± 3.3
4	44.68 ± 1.07	99.0 ± 2.4	95.8 ± 1.4
5	43.94 ± 1.42	97.4 ± 3.2	94.1 ± 0.9

Initial concentration of U(VI) = 100 mg/L, pH = 4.5 and T = 283.15 K.

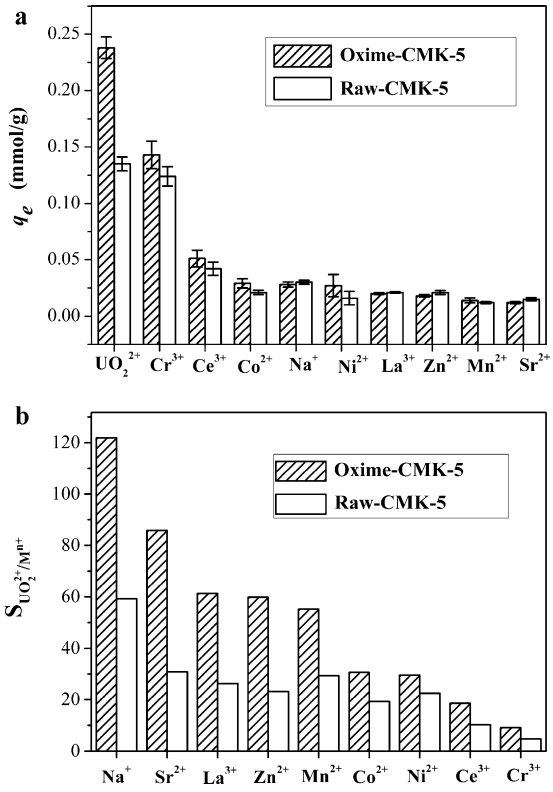

Fig. 12. (a) Competitive sorption capacity of coexistent ions and (b) selectivity coefficients ($S_{UO_2^{2+}/M}$) of Raw-CMK-5 and Oxime-CMK-5 in a simulated nuclear industry effluent, pH = 4.0, t = 120 min and T = 283.15 K.

Selectivity coefficient ($S_{UO_2^{2+}/M^{n+}}$) for uranyl ion relative to competing ions is defined as [20]:

$$S_{UO_2^{2+}/M^{n+}} = \frac{K_d^{UO_2^{2+}}}{K_d^{M^{n+}}} \quad (13)$$

where $K^d_{UO_2^{2+}}$ and $K_d^{M^{n+}}$ are distribution coefficients of uranyl ion and competing ions, respectively.

The corresponding results in Fig. 12b showed that the selectivity coefficients ($S_{UO_2^{2+}/M^{n+}}$) of Oxime-CMK-5 for all competing ions had been noticeably improved comparing with that of the matrix Raw-CMK-5, especially for Na^+, Sr^{2+}, La^{3+}, Zn^{2+} and Mn^{2+} ions, validating the graft-functionalization performed in this study was effective and Oxime-CMK-5 showed a desirable selectivity for U(VI) ions over a range of competing metal ions.

4. Conclusions

A functionalized ordered mesoporous carbon CMK-5 (Oxime-CMK-5) was prepared by covalently anchoring 4-acetophenone oxime onto CMK-5 through diazotization with high functional group contents (2.1 mmol oximes/g). The new grafting procedure

is simple and direct, and remedies the inherent shortcomings of the commonly used pre-oxidation process, such as: (i) coexistence of various oxygen-containing groups on the surface of materials responsible for unfavorable adsorption selectivity and (ii) the excessive corrosion and structural breakdown of the carbon skeleton. The selectivity and capacity of the sorbent for U(VI) uptake has been distinctly enhanced after anchoring 4-acetophenone oxime onto CMK-5 matrix. The lower activation energy and the rigidly open pore structure supported the fast sorption kinetics, and relatively higher acidity eluent (1.0 mol/L HCl) suggested the stable form of coordination between oximes on Oxime-CMK-5 and uranyl ions. Repeated sorption–desorption test indicated that the Oxime-CMK-5 sorbent can be effectively regenerated and reused for U(VI) sorption without significant loss in the sorption capability. This effective combination of the specified ligand and the mesoporous carbon matrix makes Oxime-CMK-5-based approach a promising candidate for the separation of uranium and/or other nuclides from nuclear fuel effluents as well as other related water sources.

Acknowledgment

The financial support from the National Natural Science Foundation of China (Grants 20571053 and 20871086) is gratefully acknowledged.

Appendix A. Supplementary data

Supplementary data associated with this article can be found, in the online version, at doi:10.1016/j.jhazmat.2011.03.066.

References

[1] T.P. Rao, P. Metilda, J.M. Gladis, Preconcentration techniques for uranium(VI) and thorium(IV) prior to analytical determination—an overview, Talanta 68 (2006) 1047–1064.
[2] A. Mellah, S. Chegrouche, M. Barkat, The removal of uranium(VI) from aqueous solutions onto activated carbon: kinetic and thermodynamic investigations, J. Colloid Interface Sci. 296 (2006) 434–441.
[3] S.J. Coleman, P.R. Coronado, R.S. Maxwell, J.G. Reynold, Granulated activated carbon modified with hydrophobic silica aerogel-potential composite materials for the removal of uranium from aqueous solutions, Environ. Sci. Technol. 37 (2003) 2286–2290.
[4] A.M. Starvin, T.P. Rao, Solid phase extractive preconcentration of uranium(VI) onto diarylazobisphenol modified activated carbon, Talanta 63 (2004) 225–232.
[5] Y.S. Zhao, C.X. Liu, M. Feng, Z. Chen, S.Q. Li, G. Tian, L. Wang, J.B. Huang, S.J. Li, Solid phase extraction of uranium(VI) onto benzoylthiourea-anchored activated carbon, J. Hazard. Mater. 176 (2010) 119–124.
[6] A. Schierz, H. Zanker, Aqueous suspensions of carbon nanotubes: surface oxidation, colloidal stability and uranium sorption, Environ. Pollut. 157 (2009) 1088–1094.
[7] D.D. Shao, Z.Q. Jiang, X.K. Wang, J.X. Li, Y.D. Meng, Plasma induced grafting carboxymethyl cellulose on multiwalled carbon nanotubes for the removal of UO_2^{2+} from aqueous solution, J. Phys. Chem. B 113 (2009) 860–864.
[8] Y. Xu, J.W. Zondlo, H.O. Finklea, A. Brennsteiner, Electrosorption of uranium on carbon fibers as a means of environmental remediation, Fuel Process. Technol. 68 (2000) 189–208.
[9] A.H. Lu, F. Schüth, Nanocasting: a versatile strategy for creating nanostructured porous materials, Adv. Mater. 18 (2006) 1793–1805.
[10] M. Kruk, M. Jaroniec, T.W. Kim, R. Ryoo, Synthesis and characterization of hexagonally ordered carbon nanopipes, Chem. Mater. 15 (2003) 2815–2823.
[11] H. Darmstadt, C. Roy, S. Kaliaguine, T.W. Kim, R. Ryoo, Surface and pore structures of CMK-5 ordered mesoporous carbons by adsorption and surface spectroscopy, Chem. Mater. 15 (2003) 3300–3307.
[12] S.H. Joo, S.J. Choi, I. Oh, J. Kwak, Z. Liu, O. Terasaki, R. Ryoo, Ordered nanoporous arrays of carbon supporting high dispersions of platinum nanoparticles, Nature 412 (2001) 169–172.
[13] Z.B. Lei, S.Y. Bai, Y. Xiao, L.Q. Dang, L.Z. An, G.N. Zhang, Q. Xu, CMK-5 mesoporous carbon synthesized via chemical vapor deposition of ferrocene as catalyst support for methanol oxidation, J. Phys. Chem. C 112 (2008) 722–731.
[14] X. Peng, D.P. Cao, W.C. Wang, Computational characterization of hexagonally ordered carbon nanopipes CMK-5 and structural optimization for H_2 storage, Langmuir 25 (2009) 10863–10872.
[15] M. Delamar, R. Hitmi, J. Pinson, J.M. Savbnt, Covalent modification of carbon surfaces by grafting of functionalized aryl radicals produced from electrochemical reduction of diazonium salts, J. Am. Chem. Soc. 114 (1992) 5884–5886.
[16] J.L. Bahr, J.P. Yang, D.V. Kosynkin, M.J. Bronikowski, R.E. Smalley, J.M. Tour, Functionalization of carbon nanotubes by electrochemical reduction of aryl diazonium salts: a bucky paper electrode, J. Am. Chem. Soc. 123 (2001) 6536–6542.
[17] J.L. Bahr, J.M. Tour, Highly functionalized carbon nanotubes using in situ generated diazonium compounds, Chem. Mater. 13 (2001) 3823–3824.
[18] J.L. Hudson, M.J. Casavant, J.M. Tour, Water-soluble, exfoliated, nonroping single-wall carbon nanotubes, J. Am. Chem. Soc. 126 (2004) 11158–11159.
[19] N.N. Shafa-Amry, F.I. Khalili, K.A.K. Ebraheem, M.S. Mubarak, Synthesis and chelation properties of Mannich polymers derived from piperazine and some hydroxy benzaldoximes, React. Funct. Polym. 66 (2006) 789–794.
[20] C.R. Preetha, J.M. Gladis, T.P. Rao, G. Venkateswaran, Removal of toxic uranium from synthetic nuclear power reactor effluents using uranyl ion imprinted polymer particles, Environ. Sci. Technol. 40 (2006) 3070–3074.
[21] S.H. Choi, Y.C. Nho, Adsorption of UO_2^{2+} by polyethylene adsorbents with amidoxime, carboxyl, and amidoxime/carboxyl group, Radiat. Phys. Chem. 57 (2000) 187–193.
[22] S. Das, A.K. Pandey, A.A. Athawale, V.K. Manchanda, Exchanges of uranium(VI) species in amidoxime-functionalized sorbents, J. Phys. Chem. B 113 (2009) 6328–6335.
[23] D. James, G. Venkateswaran, T.P. Rao, Removal of uranium from mining industry feed simulant solutions using trapped amidoxime functionality within a mesoporous imprinted polymer material, Micropor. Mesopor. Mater. 119 (2009) 165–170.
[24] Z.H. Luan, M. Hartmann, D.Y. Zhao, W.Z. Zhou, L. Kevan, Alumination and ion exchange of mesoporous SBA-15 molecular sieves, Chem. Mater. 11 (1999) 1621–1627.
[25] C.B. Aakeroy, A.M. Beatty, D.S. Leinen, Syntheses and crystal structures of new "extended" building blocks for crystal engineering: (pyridylmethylene) aminoacetophenone oxime ligands, Cryst. Growth Des. 1 (2001) 47–52.
[26] T. Missana, M.G. Gutiérrez, C. Maffiotte, Experimental and modeling study of the uranium (VI) sorption on goethite, J. Colloid Interface Sci. 260 (2003) 291–301.
[27] L.M. Camacho, S.G. Deng, R.R. Parra, Uranium removal from groundwater by natural clinoptilolite zeolite: effects of pH and initial feed concentration, J. Hazard. Mater. 175 (2010) 393–398.
[28] D. Borah, S. Satokawa, S. Kato, T. Kojima, Sorption of As(V) from aqueous solution using acid modified carbon black, J. Hazard. Mater. 162 (2009) 1269–1277.
[29] G.N. Manju, C. Raji, T.S. Anirudhan, Evaluation of coconut husk carbon for the removal of arsenic from water, Water Res. 32 (1998) 3062–3070.
[30] Y.S. Ho, G. McKay, Pseudo-second order model for sorption processes, Process. Biochem. 34 (1999) 451–465.
[31] I. Langmuir, The adsorption of gases on plane surfaces of glass, mica and platinum, J. Am. Chem. Soc. 40 (1918) 1361–1403.
[32] S. Aytas, M. Yurtlu, R. Donat, Adsorption characteristic of U(VI) ion onto thermally activated bentonite, J. Hazard. Mater. 172 (2009) 667–674.
[33] M.B. McBride, A critique of diffuse double layer models applied to colloid and surface chemistry, Clay. Clay. Miner. 45 (1997) 598–608.